A Constraint Enforcing Imitation Learning Approach for Optimal Operation of Unbalanced Distribution Networks

Neda Vahabzad, Pedro P. Vergara, Peter Palensky
Department of Electrical Sustainable Energy, Delft University of Technology, Delft, The Netherlands
{n.vahabzad, p.p.vergarabarrios, p.palensky}@tudelft.nl

***Abstract*—Addressing the optimal operation of modern distribution networks has become a computationally complex problem due to the integration of various distributed energy resources (DERs) and the need to handle numerous network constraints. Although data-driven methodologies show promise in addressing the non-linearity and non-convexity of such optimization problems, they often face challenges in satisfying system constraints. This paper proposes combining imitation learning (IL) with a surrogate optimization model (SOM) to minimize operational costs and active power losses, bypassing the nonlinearity in the original optimization problem while ensuring feasible solutions. The effectiveness of the proposed IL-SOM approach in accurately predicting the variables of the optimization problem is validated using a 25-bus unbalanced three-phase distribution network test case. Furthermore, the predicted variables fully comply with critical system constraints, including active and reactive power balance constraints, phase voltage, and line current magnitude limits.**

***Index Terms*—Distribution networks, Imitation learning, Optimal operation, Optimization, Surrogate model**

I. Introduction

Employing data-driven online methodologies, particularly imitation learning (IL) approaches, offers an effective strategy for addressing the complex and non-linear constraints of modern distribution systems while managing various integrated distributed energy resources (DERs), along with dynamic load profiles, renewable energy source (RES) generation patterns, and fluctuating electricity prices [1]. By emulating the functionality of nonlinear programming (NLP) solvers, IL-based methods can predict system outputs for new datasets [2]. While data-driven approaches are advantageous in bypassing nonlinearity and complexity to provide real-time predictions, they often struggle to meet system constraints, potentially resulting in less precise outcomes compared to traditional optimization solvers [3].

A. Literature review

Optimal operation problems have traditionally relied on model-driven and classical optimization methods. Numerous studies have tackled the optimal operation of DER-integrated distribution systems using conventional optimization techniques suited to the problem's complexity [4]. For instance, literature [5] presents a two-level optimization model for scheduling active distribution systems with DERs and energy storage systems. A comprehensive review of distribution system optimization problems, focusing on the algorithms, objectives, and decision variables involved, is provided in [6]. The highly non-linear, non-convex, non-differentiable, and multi-modal nature of optimal operation problems makes classical optimization methods inadequate, especially when addressing network power flow constraints and cost minimization [7]. Various linear and non-linear formulations of optimal power flow (OPF) problems in distribution systems are discussed in [8]. Accordingly, linear approximations can result in inaccuracies and infeasible solutions, while non-linear formulations struggle with computational tractability and multiple local solutions. Another crucial consideration is the distribution network configuration as highlighted in [9], which discusses a convex approximation of the AC-OPF problem based on nodal admittance matrix power flow, considering the three-phase configuration of unbalanced distribution networks.

The aforementioned complexities have led to the adoption of and data-driven techniques, leveraging historical data to extract patterns and predict system behavior [10]. Unlike traditional optimization methods, data-driven approaches provide flexibility and adaptability, enabling operators to respond effectively to system changes [11]. For instance, [12] develops real-time power dispatch approaches to maximize RES utilization, while [13] explores Neural Network (NN) models to emulate distribution system behavior in OPF problems. However, data-driven methods struggle to capture the complex relations between system parameters [14]. These algorithms encounter challenges in meeting strict operational constraints, particularly equality constraints such as power balance. To address this, [15] introduces a deep reinforcement learning algorithm that models deep NNs as mixed-integer programming (MIP) formulations, allowing for rigorous enforcement of operational constraints in real-time operations.

B. Contribution

This paper proposes a novel approach that integrates imitation learning (IL) with a surrogate optimization model (SOM) to efficiently tackle the optimal operation problem of an unbalanced three-phase distribution network. By employing an

The research is funded by the EU HORIZON 2020 MAGPIE Project no. 101036594

NN to mimic the optimization task, the IL-SOM predicts the variables for real-time, unseen input data, bypassing the original problem's complex and non-linear equations. Although the NN is trained based on optimization solver results, it does not inherently guarantee operational constraint satisfaction. To address this, the proposed approach translates the pre-trained NN into a mathematical formulation compatible with commercial solvers and enforces the desired constraints. This ensures solution feasibility by maintaining correlations between system variables and parameters, particularly considering power balance constraints, line current, and phase voltage magnitude limitations in the three-phase distribution system. Consequently, the problem shifts from a nonlinear setting to a mixed-integer quadratic framework, simplifying complexity while meeting critical operational constraints.

The remainder of the paper is organized as follows: Section II elaborates on the proposed approach, with Section II-A discussing the optimal operation problem framework and Section II-B outlining the proposed approach. In addition, Section III elaborates on simulation results and discussions. Finally, Section IV concludes the paper, summarizing the proposed approach and the obtained results.

II. Methodology

A. Optimal Operation Problem

The optimal operation of the three-phase medium-voltage distribution network, with phases denoted by $\phi, \psi \in \mathcal{F}$, nodes represented by $m, n \in \mathcal{N}$, and lines by $mn \in \mathcal{L}$, can be modeled using the equations given by (1)-(10) [16].

$$\min \sum_{\phi\in\mathcal{F}} \sum_{m\in\mathcal{N}} \Big\{ \pi^S P^S_{m,\phi} + \gamma_m (P^{DG}_{m,\phi})^2 + \beta_m P^{DG}_{m,\phi} + \alpha_m + \sum_{mn\in\mathcal{L}} \delta P^{LS}_{mn,\phi} \Big\} \tag{1}$$

subject to:

$$P^{LS}_{mn,\phi} = \sum_{\psi\in\mathcal{F}} \frac{1}{|V_{m,\psi}||V_{m,\phi}|} \Big(R'_{mn,\phi,\psi} P_{mn,\phi} P_{mn,\psi} + R'_{mn,\phi,\psi} Q_{mn,\phi} Q_{mn,\psi} + X'_{mn,\phi,\psi} P_{mn,\phi} Q_{mn,\psi} - X'_{mn,\phi,\psi} Q_{mn,\phi} P_{mn,\psi} \Big), \quad \forall mn \in \mathcal{L},\ \forall \phi \in \mathcal{F} \tag{2}$$

$$Q^{LS}_{mn,\phi} = \sum_{\psi\in\mathcal{F}} \frac{1}{|V_{m,\psi}||V_{m,\phi}|} \Big(-R'_{mn,\phi,\psi} P_{mn,\phi} Q_{mn,\psi} + R'_{mn,\phi,\psi} Q_{mn,\phi} P_{mn,\psi} + X'_{mn,\phi,\psi} P_{mn,\phi} P_{mn,\psi} + X'_{mn,\phi,\psi} Q_{mn,\phi} Q_{mn,\psi} \Big), \quad \forall mn \in \mathcal{L},\ \forall \phi \in \mathcal{F} \tag{3}$$

$$P^D_{m,\phi} = \sum_{km\in\mathcal{L}} P_{km,\phi} - \sum_{mn\in\mathcal{L}} (P_{mn,\phi} + P^{LS}_{mn,\phi}) + P^S_{m,\phi} + P^{PV}_{m,\phi} + P^{DG}_{m,\phi}, \quad \forall m \in \mathcal{N},\ \forall \phi \in \mathcal{F} \tag{4}$$

$$Q^D_{m,\phi} = \sum_{km\in\mathcal{L}} Q_{km,\phi} - \sum_{mn\in\mathcal{L}} (Q_{mn,\phi} + Q^{LS}_{mn,\phi}) + Q^S_{m,\phi}, \quad \forall m \in \mathcal{N},\ \forall \phi \in \mathcal{F} \tag{5}$$

$$P^S_{m,\phi} = Q^S_{m,\phi} = 0, \quad \forall m \in \mathcal{N},\ m \neq 0,\ \forall \phi \in \mathcal{F} \tag{6}$$

$$|V_{m,\phi}|^2 - |V_{n,\phi}|^2 = 2 \sum_{\psi\in\mathcal{F}} R'_{mn,\phi,\psi} P_{mn,\psi} + X'_{mn,\phi,\psi} Q_{mn,\psi} + \frac{1}{|V_{m,\phi}|^2} \left(\sum_{\psi\in\mathcal{F}} (R'_{mn,\phi,\psi} P_{mn,\psi} + X'_{mn,\phi,\psi} Q_{mn,\psi}) \right)^2 + \frac{1}{|V_{m,\phi}|^2} \left(\sum_{\psi\in\mathcal{F}} (R'_{mn,\phi,\psi} Q_{mn,\psi} - X'_{mn,\phi,\psi} P_{mn,\psi}) \right)^2, \quad \forall mn \in \mathcal{L},\ \forall \phi \in \mathcal{F} \tag{7}$$

$$(P_{mn,\phi})^2 + (Q_{mn,\phi})^2 \leq \overline{I}^2_{mn} |V_{m,\phi}|^2, \quad \forall mn \in \mathcal{L},\ \forall \phi \in \mathcal{F} \tag{8}$$

$$\underline{V} \leq V_{m,\phi} \leq \overline{V}, \quad \forall m \in \mathcal{N},\ \phi \in \mathcal{F} \tag{9}$$

$$\underline{P}^{DG}_{m,\phi} \leq P^{DG}_{m,\phi} \leq \overline{P}^{DG}_{m,\phi} \quad \forall m \in \mathcal{N},\ \phi \in \mathcal{F} \tag{10}$$

The objective function in (1) minimizes operational costs and active power losses. Operational costs include the cost of purchasing power from the grid at the slack bus $P^S_{m,\phi}$ at price π^S and the quadratic cost of DG unit generation [17], which depends on the decision variables $P^{DG}_{m,\phi}$. The total active power losses $P^{LS}_{mn,\phi}$ across all lines is multiplied by a cost coefficient δ to represent the corresponding cost.

The three-phase power flow constraints of the grid are defined in (2) to (9). Active and reactive power losses through the lines $P^{LS}_{mn,\phi}, Q^{LS}_{mn,\phi}$ are modeled by (2) and (3), where $R'_{mn,\phi,\psi}$ and $X'_{mn,\phi,\psi}$ are the transformed resistance and reactance between phases, defined as $R'_{mn,\phi,\psi} = R_{mn,\phi,\psi}\angle(\theta_\psi - \theta_\phi)$ and $X'_{mn,\phi,\psi} = X_{mn,\phi,\psi}\angle(\theta_\psi - \theta_\phi)$, respectively. Here, $P_{mn,\phi}$ and $Q_{mn,\phi}$ represent the active and reactive power flowing in the lines. Active and reactive power balance constraints, given by (4) and (5), ensure that the total power entering each node equals the total power leaving it. $P_{km,\phi}$ and $Q_{km,\phi}$ represent the active and reactive power from incoming lines km, while $P_{mn,\phi}$ and $Q_{mn,\phi}$ correspond to the power flowing through outgoing lines mn. Additionally, $P^D_{m,\phi}$ and $Q^D_{m,\phi}$ denote the active and reactive power demand at each node and phase. Equation (6) ensures that injected power from the external grid is zero at all buses except the slack bus. The voltage magnitude drop along the lines is given by (7), while (8), (9) and (10) impose limits on current, voltage magnitudes, and DG unit active power generation, respectively, with $\overline{I}_{mn}$, $\underline{V}$, and $\overline{V}$ as system parameters.

B. Proposed Approach

As illustrated in Fig. 1, the proposed approach includes two stages. In the first stage, an IL technique is employed to replace the original non-linear optimization problem with a NN. In the second stage, the trained NN is translated into a MIP formulation, which can be integrated with other system variables and constraints. This approach ensures a feasible solution by strictly enforcing power balance constraints, variable bounds, and the relation between NN inputs, outputs, and other variables. The details of each stage are outlined below.

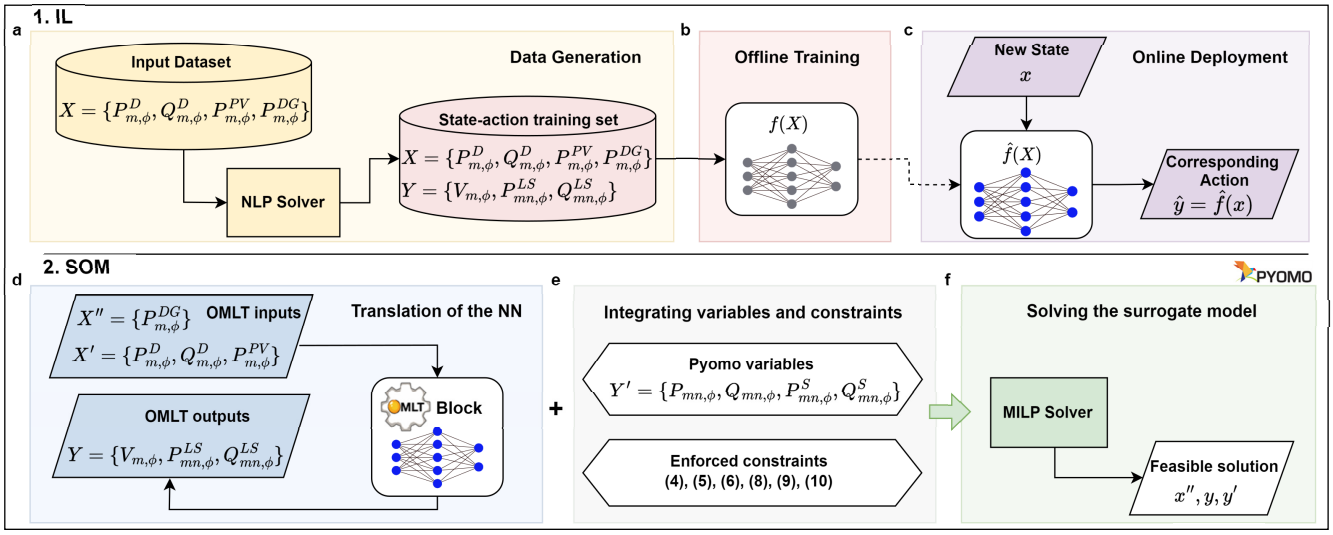

Fig. 1. Proposed IL-SOM approach: 1. IL, 2. SOM.

1) Imitation Learning: During the IL stage, a NN mimics the task of the NLP solver, thereby eliminating the need to repeatedly solve the optimization problem for new, unseen input data. This process, illustrated in part 1 of Fig. 1, consists of three steps: data generation, offline training, and online deployment. In the data generation step, a training dataset is generated by solving the original nonlinear optimization problem using a NLP solver for a large input dataset. The effectiveness of the IL approach is closely tied to the size of the training dataset, with larger datasets leading to more accurate IL models [18]. Vector X in Fig. 1, represents input states including active and reactive power demand, PV power generation, and the active power generation of DG units. The reasoning behind the inclusion of $P^{DG}_{m,\phi}$, a variable of the optimization problem, as an input state is elaborated in Section II-B2. The output action set Y includes the phase voltage magnitudes of all buses and the active and reactive power losses of all lines. In the offline training phase, a NN designed for regression tasks is trained, and validated using the $X - Y$ training set, generated in Step (a). Through extensive training, the NN approximates the function employed by the NLP solver to map input states to their corresponding actions. This acquired policy is subsequently utilized in the online deployment step, where the trained NN predicts the defined state variables for unseen data encountered by the system.

2) Surrogate Optimization Model: The NN introduced in Section II-B1 faces challenges in providing feasible solutions that fully comply with the optimization constraints. As shown in part 2 of Fig. 1, the second stage of the proposed approach addresses this issue by incorporating hard constraints and variable bounds into the IL process. This is achieved by embedding the NN within the Pyomo environment[1] using the Optimization and Machine Learning Toolkit (OMLT)[2]. OMLT simplifies this process by encapsulating NN components within a Pyomo block, referred to as the OMLT block, which includes an MIP formulation for the NN translation.

The OMLT block, shown in Step (d) of Fig. 1, encapsulates the trained NN within the Pyomo environment, defined by its inputs and outputs, denoted as X and Y of the $X - Y$ training set. This approach allows users to focus on the NN's input/output structure without delving into the detailed equations. When optimizing OMLT blocks, the solver finds optimal values for inputs within specified bounds to ensure feasible solutions considering the objective function and the enforced constraints. Fixed parameters, denoted by X' including $P^D_{m,\phi}$, $Q^D_{m,\phi}$, and $P^{PV}_{m,\phi}$, remain constant, while the optimal value of X'' comprising $P^{DG}_{m,\phi}$, is computed within predefined bounds given to the OMLT block. This explains why $P^{DG}_{m,\phi}$ is included as a feature in the NN for the IL process in Section II-B1.

In Step (e) of the proposed SOM, OMLT inputs X',X'', and output Y, along with additional variables represented by Y' (including active and reactive power flowing in lines, and the active and reactive power injected from the slack bus) are integrated as Pyomo variables into the broader optimization problem. To maintain the relation between the input and output variables of the OMLT block, which are the features and labels of the NN, and the Pyomo variables, the constraints of the original optimization problem can be involved. While the same objective function, which minimizes operational costs and active power losses, is employed, the constraints (4), (5), (6), (8), (9), and (10) are enforced to avoid ending up with an MINLP problem. Finally, the constraint-enforcing IL-SOM is effectively handled in Pyomo using a GUROBI solver, as shown in step (f).

III. Simulation Results and Discussions

The proposed approach is tested on a 25-bus, three-phase medium-voltage distribution network, based on the configuration outlined in [16], with modifications applied to the

[1]https://pyomo.readthedocs.io
[2]https://omlt.readthedocs.io

included DERs, as shown in Fig. 2. The active generation capacities of the DERs at each bus, including five DG and ten PV units, are listed in Table I.

Both the original and the surrogate optimization problems

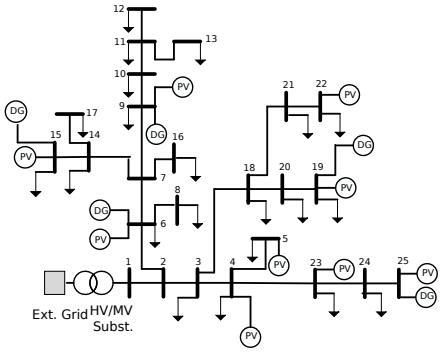

Fig. 2. The considered medium-voltage distribution network.

are formulated in the Pyomo environment, a Python-based tool for modeling optimization problems. The IPOPT [3], and GUROBI [4] solvers are used to deal with the original and surrogate optimization problems, respectively.

A random input dataset is generated using (11) and the base active/reactive demand and PV generation capacity at each node and phase [19]. Here, $H_{m,\phi}$ denotes the base data, H^{dev} is the maximum deviation from the base value (set at 0.005), and $n(i)$ is a random sample from the base data distributions. The NN is trained based on the results from solving the original NLP problem for 3,000 randomly generated inputs. This dataset size balances training time and performance, achieving strong regression metrics: MSE of 0.01, MAE of 0.09, RMSE of 0.12, and R^2 score of 0.98. These results indicate the designed NN's effectiveness in capturing data patterns and making accurate predictions. The NN in the IL procedure is implemented in Keras with a single hidden layer of 100 neurons.

$$H_{i,m,\phi} = (1 + n(i) \times H^{\text{dev}}) H_{m,\phi} \tag{11}$$

Further considerations involve defining the scaler object used in data preparation during the training of the NN. This addresses the challenge of training the NN with scaled features and labels, while the embedded NN operates in unscaled space in the optimization framework. Additionally, a suitable formulation object must be utilized to translate the NN from its higher-level representation (ONNX or Keras) to fit within the optimization framework. For this purpose, ReluBigMFormulation [20] is selected when replacing the NN with the OMLT block, as the trained NN uses the ReLU activation function in its hidden layer, resulting in a MILP problem solvable by the GUROBI solver.

Figure 3 presents the distribution of the NN's target labels ($V_{m,\phi}$, $P^{LS}_{mn,\phi}$, and $Q^{LS}_{mn,\phi}$), calculated with the original optimization (OPT), IL, and IL-SOM approaches for a set

[3]https://coin-or.github.io/Ipopt

[4]https://www.gurobi.com

TABLE I
DER GENERATION CAPACITIES

m	4	5	6	9	14	15	19	22	23	25
$\overline{P}^{PV}_{m,\phi}$ (kW)	15	30	12	20	15	40	20	20	15	10
$\overline{P}^{DG}_{m,\phi}$ (kW)	0	0	40	20	0	10	30	0	0	30

TABLE II
STATISTICAL MEASUREMENTS OF THE OBJECTIVE FUNCTION

Statistical Measures (€)	mean	std	median
OPT	105375.3	9219.51	106067.25
IL-SOM	74673.81	4546.59	71858.41

of unseen data. The boxplots reveal that both IL and IL-SOM predictions closely align with the actual values obtained from the OPT model, highlighting the effectiveness of these methods in accurately following the NLP solver's policy for variable calculation.

Additionally, Fig. 4 illustrates the average of the absolute difference between active power generation and demand for each phase and bus within the considered three-phase unbalanced distribution network over the unseen data. It is obvious that the power imbalance is always zero with the proposed IL-SOM approach, unlike the values obtained using only the IL approach. This highlights that despite the alignment of the labels generated solely by the IL method to the actual labels calculated by the OPT model, they do not ensure the active power balance constraint. In contrast, outputs from the IL-SOM approach consistently meet this constraint across all buses and phases for all unseen input data.

Various statistical measurements such as mean, median, and standard deviation are given by Table II to compare the objective values in OPT and IL-SOM approaches obtained

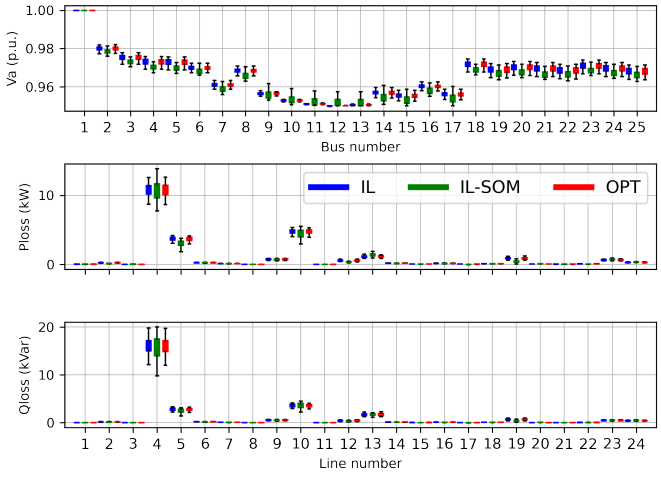

Fig. 3. Distribution of NN target labels across buses over unseen datasets; via OPT (red), IL (blue), IL-SOM (green) approaches.

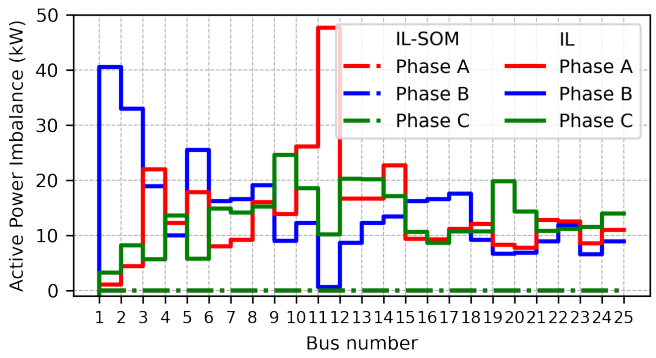

Fig. 4. Average active power imbalance at each bus and phase over unseen datasets; with IL and IL-SOM approaches.

for a set of unseen data. Furthermore, the IL-SOM approach achieves a longer solving time (47.5 seconds) than the NLP solver (14.5 seconds) for the same set of unseen data. However, the strength of the proposed approach lies in its ability to bypass nonlinearity and enforce constraints effectively, rather than in reducing solving time. Additionally, the increased solving time can result from factors such as overhead costs associated with OMLT blocks or other code-related considerations, which are beyond the scope of this paper.

IV. Conclusion

Addressing the optimal operation problem in distribution networks is vital to its safe and efficient operation; and managing DERs effectively. However, tackling this issue in real-time applications is complex due to the nonlinear AC OPF constraints of the grid, and numerous decision variables. This paper introduced an IL-based approach that overcomes these nonlinearities by using a neural network to predict the variables of the optimization problem. The implemented IL model demonstrated proficiency in accurately predicting the desired labels, achieving an MSE of 0.01 and an R2 score of 0.98. Furthermore, by integrating the pre-trained NN into the optimization framework, a surrogate optimization model is formulated that is able to follow the original objective function and enforce constraints. Testing this approach on a 25-bus unbalanced three-phase distribution network confirmed its adherence to critical constraints, such as active and reactive power balance, and line current and voltage magnitude limits. Future work could focus on reducing the solving time of the proposed IL-SOM approach to enable its application in larger optimization problems.

References

[1] W. Ahmed *et al.*, "Machine learning based energy management model for smart grid and renewable energy districts," *IEEE Access*, vol. 8, pp. 185059-185078, 2020.

[2] S. Gao, C. Xiang, M. Yu, K. T. Tan, and T. H. Lee, "Online optimal power scheduling of a microgrid via imitation learning," *IEEE Trans. Smart Grid*, vol. 13, no. 2, pp. 861-876, Oct 2021.

[3] S.L. Brunton*et al.*, "Data-driven aerospace engineering: reframing the industry with machine learning," *AIAA Journal*, vol. 59, no. 8, pp. 2820-2847, 2021.

[4] H. Xiao, W. Pei, Z. Dong, L. Kong, and D. Wang, "Application and comparison of metaheuristic and new metamodel based global optimization methods to the optimal operation of active distribution networks," *Energies*, vol. 11, no. 1, p. 85, 2017.

[5] H. Zakernezhad, M. S. Nazar, M. Shafie-khah, and J. P. S. Catalão, "Optimal scheduling of an active distribution system considering distributed energy resources, demand response aggregators and electrical energy storage," *Appl. Energy*, vol. 314, May 2022.

[6] A. R. Jordehi, "Optimisation of electric distribution systems: A review," *Renewable and Sustainable Energy Reviews*, vol. 51, pp. 1088-1100, Nov 2015.

[7] M. Wang, T. Zhang, P. Wang, and X. Chen, "An improved harmony search algorithm for solving day-ahead dispatch optimization problems of integrated energy systems considering time-series constraints," *Energy and Buildings*, vol. 229, 2020.

[8] R. R. Jha *et al.*, "Distribution grid optimal power flow (D-OPF): modeling, analysis, and benchmarking," *IEEE Trans. Power Syst.*, vol. 38, no. 4, pp. 3654-3668, July 2023.

[9] J. D. Watson, N. R. Watson, and I. Lestas, "Optimized dispatch of energy storage systems in unbalanced distribution networks," *IEEE Trans. Sustainable Energy*, vol. 9, no. 2, pp. 639-650, April 2018.

[10] C. Ren and Y. Xu, "A fully data-driven method based on generative adversarial networks for power System dynamic security assessment with missing data," *IEEE Trans. Power Syst.*, vol. 34, no. 6, pp. 5044-5052, Nov 2019.

[11] A. Almaghrebi, F. Aljuheshi, M. Rafaie, K. James, and M. Alahmad, "Data-driven charging demand prediction at public charging stations using supervised machine learning regression methods," *Energies*, vol. 13, no. 16, p. 4231, 2020.

[12] Z. Li, F. Qiu, and J. Wang, "Data-driven real-time power dispatch for maximizing variable renewable generation," *Appl. Energy*, vol. 170, pp. 304-313, 2016.

[13] D. K. Mahto, V. K. Saini, A. Mathur, R. Kumar, and A. Saxena, "Data driven approach for optimal power flow in distribution network," *2021 5th International Conference on Information Systems and Computer Networks (ISCON)*, Mathura, India, 2021, pp. 1-6.

[14] X. Lei, Z. Yang, J. Yu, J. Zhao, Q. Gao, and H. Yu, "Data-driven optimal power flow: A physics-informed machine learning approach," *IEEE Trans. Power Syst.*, vol. 36, no. 1, pp. 346-354, Jan 2021.

[15] H. Shengren, P. P. Vergara, E. M. Salazar Duque, and P. Palensky, "Optimal energy system scheduling using a constraint-aware reinforcement learning algorithm," *International Journal of Electrical Power and Energy Systems*, vol. 152, p. 109230, 2023.

[16] P. P. Vergara, J. C. López, M. J. Rider, and L. C. Da Silva, "Optimal operation of unbalanced three-phase islanded droop-based microgrids," *IEEE Trans. Smart Grid*, vol. 10, no. 1, pp. 928-940.

[17] K. Kusakana and H. J. Vermaak, "Hybrid diesel generator/renewable energy system performance modeling," *Renewable Energy*, vol. 67, pp. 97-102, 2014.

[18] A. Althnian, D. AlSaeed, H. Al-Baity, A. Samha, A. B. Dris, N. Alzakari, A. Abou Elwafa, and H. Kurdi, "Impact of dataset size on classification performance: an empirical evaluation in the medical domain," Appl. Sci., vol. 11, no. 2, p. 796, 2021.

[19] D. E. Olivares, C. A. Cañizares, and M. Kazerani, "A centralized energy management system for isolated microgrids," *IEEE Trans. Smart Grid*, vol. 5, no. 4, pp. 1864–1875, 2014.

[20] F. Ceccon, J. Jalving, J. Haddad, A. Thebelt, C. Tsay, C. D. Laird, and R. Misener, "OMLT: Optimization and machine learning toolkit," *J. Mach. Learn. Res.*, vol. 23, no. 349, pp. 1-8.